Neuron, Vol. 23, 593–605, July, 1999, Copyright ©1999 by Cell Press

Syntaxin 1A Interacts with Multiple Exocytic Proteins to Regulate Neurotransmitter Release In Vivo

Mark N. Wu,*† Tim Fergestad,‖ Thomas E. Lloyd,*† Yuchun He,† Kendal Broadie,‖ and Hugo J. Bellen*†‡§#
*Department of Cell Biology
†Howard Hughes Medical Institute
‡Department of Molecular and Human Genetics
§Division of Neuroscience
Baylor College of Medicine
Houston, Texas 77030
‖Department of Biology
University of Utah
Salt Lake City, Utah 84112

Summary

Biochemical studies suggest that syntaxin 1A participates in multiple protein–protein interactions in the synaptic terminal, but the in vivo significance of these interactions is poorly understood. We used a targeted mutagenesis approach to eliminate specific syntaxin binding interactions and demonstrate that *Drosophila* syntaxin 1A plays multiple regulatory roles in neurotransmission in vivo. Syntaxin mutations that eliminate ROP/Munc-18 binding display increased neurotransmitter release, suggesting that ROP inhibits neurosecretion through its interaction with syntaxin. Syntaxin mutations that block Ca^{2+} channel binding also cause an increase in neurotransmitter release, suggesting that syntaxin normally functions in inhibiting Ca^{2+} channel opening. Additionally, we identify and characterize a syntaxin Ca^{2+} effector domain, which may spatially organize the Ca^{2+} channel, cysteine string protein, and synaptotagmin for effective excitation–secretion coupling in the presynaptic terminal.

Introduction

Fusion of vesicles with their target membranes involves interaction of synaptobrevin homologs in the vesicle with SNAP-25 and syntaxin homologs in the target membrane (Jahn and Hanson, 1998). These three proteins form a stable, SDS-resistant complex, called the SNARE complex or core complex (Sollner et al., 1993a; Hayashi et al., 1994). Genetic and toxin experiments that affect proteins of the core complex block neurotransmitter release and cause accumulation of docked vesicles, suggesting that the core complex functions after vesicle docking (Hunt et al., 1994; Broadie et al., 1995; Schulze et al., 1995; Sweeney et al., 1995). Structural studies reveal that the core complex forms a parallel four-helix bundle, which is postulated to act as a mechanism to pull vesicular and target membranes close together to mediate membrane fusion (Hanson et al., 1997; Lin and Scheller, 1997; Sutton et al., 1998). Indeed, the core complex alone is sufficient to mediate fusion of lipid micelles in vitro (Weber et al., 1998).

Syntaxin appears to be a central coordinator of this exocytosis machinery. In *Drosophila*, for example, *syntaxin* mutants completely lack both evoked and spontaneous neurotransmission and also fail to secrete epidermal cuticle, indicating that *Drosophila* Syntaxin (by convention, *Drosophila* proteins are capitalized) is essential for both neuronal and nonneuronal secretion (Schulze et al., 1995). Moreover, at the synapse, syntaxin 1A has more binding partners than any other presynaptic protein. In addition to synaptobrevin and SNAP-25, syntaxin 1A binds at least nine other neuronal proteins, including Munc-18/n-Sec1, Ca^{2+} channels, synaptotagmin, complexins, α-SNAP, rsec6/rsec8, CIRL/latrophilin, tomosyn, and Munc-13 (Bennett et al., 1992; Hata et al., 1993; Sollner et al., 1993b; Sheng et al., 1994; Chapman et al., 1995; McMahon et al., 1995; Hsu et al., 1996; Betz et al., 1997; Krasnoperov et al., 1997; Fujita et al., 1998). The interactions of these proteins with syntaxin likely play modulatory roles in neurosecretion, but the precise functions of these protein–protein interactions are controversial.

One intriguing interaction is the binding of syntaxin 1A to members of the Munc-18/n-Sec1/ROP family (Hata et al., 1993; Pevsner et al., 1994a). Genetic studies of Sec1 homologs have shown that these proteins perform a positive function in exocytosis, as mutants show severe defects in both neuronal and nonneuronal secretion (Novick et al., 1980; Harrison et al., 1994; Wu et al., 1998). Therefore, it has been suggested that the syntaxin-Munc-18/n-Sec1 interaction positively regulates secretion (Bajjalieh and Scheller, 1995; Dresbach et al., 1998). However, more recent studies of ROP, the *Drosophila* Sec1 homolog, have demonstrated that this protein also performs an inhibitory role in exocytosis in vivo (Schulze et al., 1994; Wu et al., 1998). Hence, it is unclear whether the positive or inhibitory function of ROP/n-sec1 is mediated by its interaction with Syntaxin or with other proteins.

Another potential regulatory interaction is the binding of syntaxin 1A to synaptic N-, P-, and Q-type calcium channels, at the cytoplasmic loop between domains II and III, called the synprint site (Sheng et al., 1994, 1996). A functional correlate of this binding was proposed on the basis of synprint peptide competition experiments, which suggested that inhibiting the syntaxin–Ca^{2+} channel interaction caused a reduction in evoked synaptic transmission, with an increase in asynchronous release. Thus, this interaction was proposed to tether the core complex at Ca^{2+} channels in order to localize the fusion machinery near the site of Ca^{2+} influx and potentiate neurotransmission (Mochida et al., 1996; Rettig et al., 1997). However, studies in which syntaxin 1A was expressed in *Xenopus* oocytes showed that the protein functions to inhibit Ca^{2+} channels (Bezprozvanny et al., 1995; Wiser et al., 1996). In this context, syntaxin may function to reduce random or unregulated Ca^{2+} channel openings, and loss of this function would be postulated to lead to enhanced neurotransmitter release. Therefore,

#To whom correspondence should be addressed (e-mail: hbellen@bcm.tmc.edu).

a syntaxin–Ca^{2+} channel interaction has been suggested to play at least two roles in neurotransmitter release: a potentiating tethering function and an inhibitory regulatory function.

These controversies have so far proven refractory to in vivo analyses. Perturbations of syntaxin function by antibody, peptide, or toxin injection (O'Connor et al., 1997; Marsal et al., 1997; Sugimori et al., 1998) or by available mutations in yeast, *C. elegans*, and *Drosophila* (Schulze et al., 1995; Nichols et al., 1997; Saifee et al., 1998) all cause a similar phenotype: a block in secretion. Since synaptic vesicle exocytosis likely involves several Syntaxin-mediated protein–protein interactions, understanding the mechanisms underlying neurotransmitter release requires a detailed understanding of the functions of specific protein interactions with Syntaxin in vivo. Therefore, we used a targeted mutagenesis approach to eliminate specific Syntaxin interactions and perform a structure–function analysis in vivo. Here, we provide evidence that Syntaxin performs multiple functions in exocytosis, as different mutations in *syntaxin* cause dramatically different effects on neurotransmitter release. We show that the core complex is essential for neurotransmission. Our data suggest that the ROP–Syntaxin interaction and the Syntaxin–Ca^{2+} channel interaction both play inhibitory, not positive, roles in neurotransmitter release. Finally, our studies identify a novel C-terminal "Ca^{2+} effector domain" in Syntaxin. This Ca^{2+} effector domain binds to and may spatially organize the Ca^{2+} channel, cysteine string protein (a protein implicated in regulating presynaptic Ca^{2+} channels), and Synaptotagmin (a putative Ca^{2+} sensor) and is specifically required for efficient excitation–secretion coupling in vivo.

Results

Binding Analysis of the H3 Domain of *Drosophila* Syntaxin 1A

To dissect the putative functions of Syntaxin in vivo, we generated partial loss-of-function mutations in *syntaxin 1A* (*syx*). As this gene is refractory to standard mutagenesis with EMS (ethylmethylsulfonate) (Schulze and Bellen, 1996), we used a site-directed mutagenesis approach to interfere with specific protein–protein interactions. As shown in Figure 1, Syntaxin 1A has four coiled-coil domains (H1/HA, H2/HB, HC, and H3; Kee et al., 1995; Fernandez et al., 1998). All binding partners, with one exception (Munc-13), bind the C-terminal third of Syntaxin including the H3 domain (Chapman et al., 1994, 1995; Sheng et al., 1994; Kee et al., 1995; Betz et al., 1997). We thus focused on a structure–function analysis of the H3 domain.

As shown in Figure 1, four mutations in the *syx* H3 domain were generated: two deletions ($syx^{H3\text{-}N}$ and $syx^{H3\text{-}C}$) and two point mutations (syx^{2} and syx^{3}). The $syx^{H3\text{-}N}$ deletion removes the majority of the N-terminal region of the H3 domain (amino acids 204–250), whereas the $syx^{H3\text{-}C}$ deletion removes the highly basic C-terminal 14 amino acids of the H3 domain (amino acids 253–267). For the syx^{2} and syx^{3} constructs, point mutations were made in the hydrophobic layers, which appear to be important for specific protein–protein interactions and

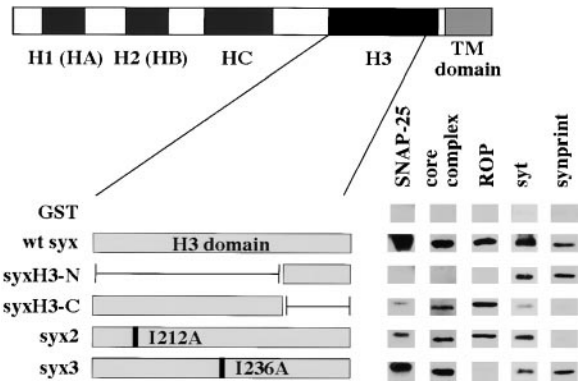

Figure 1. Binding Analysis of the H3 Domain of *Drosophila* Syntaxin

Above, a schematic is shown, demonstrating the four coiled-coil domains of Syntaxin—H1 (HA), H2 (HB), HC, and H3. The transmembrane (TM) domain is at the C-terminal end of the protein. The ability of GST fusion proteins to interact with SNAP-25 (n = 3), ROP (n = 2), Synaptotagmin (Syt) (n = 5), and synprint (n = 3) was determined by ECL blotting (Amersham). Core complex formation (n = 3) was assessed by incubating the GST fusion proteins in the presence of both Syb and SNAP-25 and assaying for the presence of Syb after boiling.

for core complex stability (Kee et al., 1995; Sutton et al., 1998; Chen et al., 1999). Specifically, the syx^{2} point mutation falls in a region thought to be required for SNAP-25 binding, and the amino acid targeted by the syx^{3} mutation was shown to be important for binding to n-Sec1/Munc-18.

To define the binding defects caused by the *syx* mutations, we performed GST pulldown assays. In this assay, GST alone, wild-type GST–Syx, or mutant GST–Syntaxins were immobilized on glutathione–Sepharose beads and incubated with target proteins. The binary Syb–Syx interaction is easily disrupted, as every *syx* mutation reveals a strong reduction if not complete absence of Syb binding (data not shown). This finding is consistent with studies using vertebrate proteins (Hayashi et al., 1994; Kee et al., 1995) and does not appear physiologically relevant, since certain mutants display robust neurotransmission (see below). We therefore tested core complex formation by assaying Syb binding in the presence of SNAP-25 (Figure 1). The $syx^{H3\text{-}N}$ deletion abolishes formation of the core complex, while GST–$Syx^{H3\text{-}C}$ can form a core complex, although less efficiently than wild-type GST–Syx. The syx^{2} and syx^{3} point mutants are both capable of forming core complexes.

Next, we examined the abilities of the GST–Syx mutant proteins to bind ROP, Synaptotagmin (Syt), and the synprint site of the N-type Ca^{2+} channel. As shown in Figure 1, GST–$Syx^{H3\text{-}N}$ shows an abolishment of ROP binding, but binds Synaptotagmin and synprint. Conversely, the GST–$Syx^{H3\text{-}C}$ deletion can bind ROP, but shows a severe reduction in Synaptotagmin and synprint binding, relative to wild-type GST–Syx. Therefore, these findings suggest that the N-terminal region of the H3 domain is essential for core complex formation and ROP binding, while the C-terminal 14 amino acids of the H3 domain are required for efficient binding to Synaptotagmin and synprint.

Binding analysis of the point mutations show that the

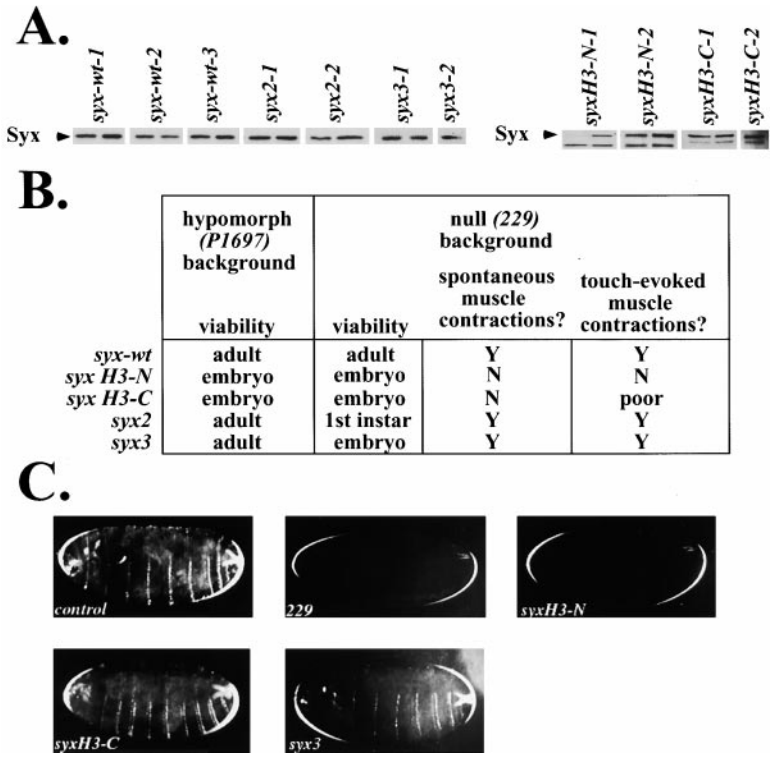

	hypomorph (P1697) background	null (229) background		
	viability	viability	spontaneous muscle contractions?	touch-evoked muscle contractions?
syx-wt	adult	adult	Y	Y
syx H3-N	embryo	embryo	N	N
syx H3-C	embryo	embryo	N	poor
syx2	adult	1st instar	Y	Y
syx3	adult	embryo	Y	Y

Figure 2. Generation of Novel Syntaxin Mutations In Vivo

(A) Westerns of single embryos aged 21–22 hr AEL (after egg lay) probed for Syntaxin. syx^{wt}, syx^{2}, and syx^{3} embryos in the homozygous null background (e.g., *y w*; syx^{2}/syx^{2}; syx^{229}/syx^{229}) were run on the same gel with control embryos, in order to assess relative levels. For $syx^{H3\text{-}N}$ and $syx^{H3\text{-}C}$, embryos in the heterozygote null background were analyzed (e.g., *y w*; $syx^{H3\text{-}N}/syx^{H3\text{-}N}$; syx^{229}/*TM6*). Hence, the higher band represents wild-type Syx, while the lower band represents the shorter mutant Syx protein.

(B) Lethality phase and ability to undergo spontaneous and touch evoked embryonic muscle contractions (for 26–30 hr AEL embryos) of different *syntaxin* mutants. Mutant embryos were identified by either using outcrossed lines or by the absence of the GFP balancer.

(C) Cuticles from 22–23 hr AEL embryos were prepared as described (Ashburner, 1990) and imaged at 10× using darkfield microscopy. Anterior is to the left. In the wild-type control (*y w*) embryo, cuticle structures such as mouthhooks (anterior) and posterior spiracles are observed. syx^{wt} embryos resembled *y w* embryos (data not shown). Denticle belts are observed in control embryos, but not in syx^{229} null mutants or $syx^{H3\text{-}N}$ embryos. In some cases, denticle belts for $syx^{H3\text{-}C}$ mutants appear thinner and somewhat irregular compared to wild type. The presence of posterior spiracles in syx^{229} and $syx^{H3\text{-}N}$ embryos indicates that they are fertilized.

syx^{2} and syx^{3} mutations selectively disrupt binding to different Syntaxin partners. The syx^{3} mutation specifically abolishes ROP binding to Syntaxin. Surprisingly, the most striking binding defect caused by the syx^{2} point mutation is an abolishment of binding to synprint. This effect is specific for syx^{2}, as GST–Syx^{3} and GST–$Syx^{H3\text{-}N}$ are capable of binding synprint. Curiously, syx^{2} lies within a domain not required for synprint binding, as demonstrated by GST–$Syx^{H3\text{-}N}$, suggesting that the point mutation induces a conformational change in the C-terminal region of the H3 domain. Although unexpected, structural studies have shown that amino acid substitutions can cause long-range effects on binding properties of a protein (Brown et al., 1993; Fisher et al., 1998). In contrast, the point mutations do not significantly affect Synaptotagmin binding, when compared to wild-type GST–Syx. These data confirm that, similar to vertebrate syntaxin 1A, the H3 domain of *Drosophila* Syntaxin is important for core complex formation and binding to ROP, Synaptotagmin, and synprint. Further, our in vitro findings show that specific Syntaxin protein interactions can be selectively blocked by point mutations in the H3 domain.

Generation of Novel *syntaxin* Mutations

To address the in vivo effects of the $syx^{H3\text{-}N}$, $syx^{H3\text{-}C}$, syx^{2}, and syx^{3} mutations, we introduced these mutations into flies. Since a 13.5 kb genomic fragment containing *syx* (syx^{wt}) can rescue a null allele (syx^{229}) to adult viability, each mutation was introduced in the 13.5 kb fragment, sequenced, and used to generate transgenic flies. The wild-type genomic rescue construct was used as control (syx^{wt}). Transgenic flies bearing the mutant and wild-type constructs were then crossed into syx^{P1697} (hypomorph) and syx^{229} (null) backgrounds. To control for position effects, several independent transgenic lines were established for each mutant construct. Single embryo Westerns (Figure 2A) showed that $Syx^{H3\text{-}N}$, Syx^{2}, and Syx^{3} mutant proteins are produced at levels similar to Syx^{wt} controls. However, $Syx^{H3\text{-}C}$ mutant protein is expressed relatively poorly, compared to other mutants. Different transgenic lines for the same mutation expressed similar amounts of mutant Syntaxin protein, indicating that position effects did not significantly affect protein levels. Immunocytochemical stainings indicated that the mutant Syntaxins are expressed in a spatial and temporal pattern indistinguishable from wild-type (data not shown). In addition, to determine if different mutant Syntaxins somehow altered the levels of other synaptic proteins, we performed Western analysis for syx^{wt}, $syx^{H3\text{-}N}$, $syx^{H3\text{-}C}$, syx^{2}, and syx^{3} embryos and found that the levels of ROP, CSP, Synaptotagmin, and SNAP-25 were unchanged in mutants, relative to controls (data not shown).

As shown in Figure 2B, mutants and wild-type controls were first assessed for their ability to rescue the lethality of syx^{P1697} and syx^{229}. The deletion mutations are the most severe, as $syx^{H3\text{-}N}$ and $syx^{H3\text{-}C}$ mutants are embryonic lethal in both the null and partial loss-of-function background. In contrast, the point mutations cause milder phenotypes, allowing animals to live to adulthood in the

hypomorphic background, but not in the null background. Since different transgenic lines bearing the same mutation have similar lethal phases (data not shown) and protein expression levels, the phenotypes discussed below result from the mutations, not from position effects. All further characterization of syx^{wt} and specific mutations were carried out in the absence of wild-type zygotic Syntaxin, that is, in the homozygote null background (syx^{229}/syx^{229}).

Wild-type *Drosophila* embryos undergo peristaltic muscular contractions prior to hatching. As shown in Figure 2B, $syx^{H3\text{-}N}$ and $syx^{H3\text{-}C}$ mutants do not undergo spontaneous muscle contractions, suggesting that neurotransmission is severely affected. However, in response to tactile stimulation, $syx^{H3\text{-}C}$ mutants are capable of weak, local contractions, whereas $syx^{H3\text{-}N}$ mutants fail to respond. In contrast, syx^{2} and syx^{3} mutant animals are capable of spontaneous peristaltic contractions and robust touch response. These data suggest that synaptic transmission is more severely affected in $syx^{H3\text{-}N}$ and $syx^{H3\text{-}C}$ mutants than in syx^{2} or syx^{3} mutants.

In wild-type *Drosophila* embryos, epidermal cells secrete a cuticle apically (Martinez Arias, 1993). The presence of cuticle can easily be visualized by the presence of cuticular denticle belts, which is a convenient assay for nonneuronal secretion. *syx* null mutants (syx^{229}) fail to secrete cuticle and completely lack denticles, indicating an essential role for Syntaxin in nonneuronal secretion (Schulze et al., 1995). We assayed the ability of our different *syx* mutants to carry out nonneuronal secretion. All mutants except $syx^{H3\text{-}N}$ are capable of secreting cuticle normally (Figure 2C), suggesting that the inability to form core complexes blocks nonneuronal secretion. Moreover, perturbations of specific syntaxin protein interactions, most importantly the Syntaxin–ROP interaction, does not appear to affect nonneuronal secretion.

The Core Complex Is Essential for Vesicle Fusion

We next assayed regulated exocytosis at the synaptic terminal in our *syntaxin* mutants. As shown in Figure 3A, the $syx^{H3\text{-}N}$ deletion abolishes core complex formation. We investigated synaptic transmission in $syx^{H3\text{-}N}$ mutants using whole-cell patch-clamp analysis at the embryonic neuromuscular junction (NMJ). Three different wild-type transgenic controls ($syx^{wt\text{-}1}$, $syx^{wt\text{-}2}$, $syx^{wt\text{-}3}$) showed robust evoked neurotransmission (Figures 3B and 3C). However, as shown in Figures 3B–3D, evoked and spontaneous neurotransmission is completely abolished in $syx^{H3\text{-}N}$ animals (n = 16), showing that the $syx^{H3\text{-}N}$ mutant phenotype is identical to that of *syntaxin* null mutants (Broadie et al., 1995; Schulze et al., 1995). As shown for the *syx* null mutant (Broadie et al., 1995), direct glutamate pressure ejection at the synapse of $syx^{H3\text{-}N}$ mutants reveals that the postsynaptic muscles respond normally to neurotransmitter (data not shown), indicating that the block in neurotransmission is presynaptic in nature. The complete absence of neurotransmitter release in $syx^{H3\text{-}N}$ mutants, taken together with the absence of nonneuronal secretion in these mutants, suggests that the core complex is essential for both neuronal and nonneuronal vesicular fusion.

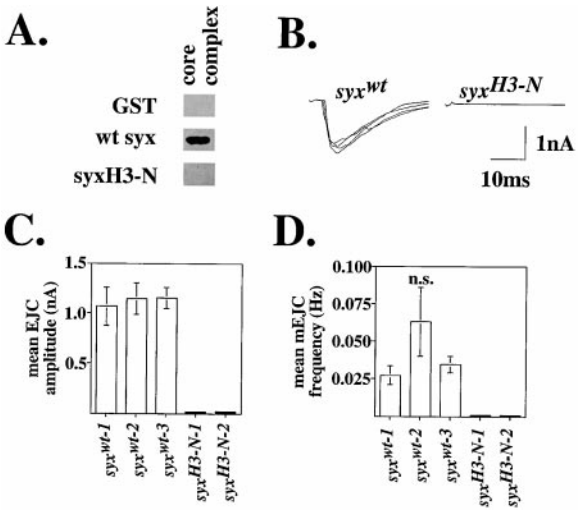

Figure 3. The Core Complex Is Essential for Neurotransmission

(A) The $syx^{H3\text{-}N}$ deletion abolishes core complex formation. The ability of GST, GST–Syx, and GST–$Syx^{H3\text{-}N}$ to form core complexes is shown.

(B) Evoked neurotransmitter release in syx^{wt} and $syx^{H3\text{-}N}$. Traces show representative EJCs after nerve stimulation at basal stimulation frequencies (1 Hz) from these lines.

(C) Mean EJC amplitudes of $syx^{wt\text{-}1}$ (n = 5), $syx^{wt\text{-}2}$ (n = 9), $syx^{wt\text{-}3}$ (n = 5), $syx^{H3\text{-}N\text{-}1}$ (n = 8), and $syx^{H3\text{-}N\text{-}2}$ (n = 8) are plotted.

(D) Mean mEJC frequency is plotted for $syx^{wt\text{-}1}$ (n = 4), $syx^{wt\text{-}2}$ (n = 4), $syx^{wt\text{-}3}$, (n = 3), $syx^{H3\text{-}N\text{-}1}$ (n = 8), and $syx^{H3\text{-}N\text{-}2}$ (n = 8) embryos. Although mEJC frequency is somewhat increased in $syx^{wt\text{-}2}$ compared to other controls, this increase is not statistically significant (n.s.).

The ROP–Syntaxin Interaction Inhibits Synaptic Transmission

To define the function of the Syntaxin–ROP complex, we focused on a phenotypic analysis of the syx^{3} mutant, since the syx^{3} mutation selectively disrupts the Syntaxin–ROP interaction (Figures 1A and 4A). First, since the syx^{3} mutation affects a hydrophobic residue that may be important for core complex stability, we tested the heat lability of SDS-resistant core complexes containing GST–Syx^{3}. As shown in Figure 4B, the syx^{3} mutation does not significantly alter core complex stability relative to wild-type control, although the levels of SDS-resistant core complexes are somewhat reduced at 54°C for GST–Syx^{3} compared to wild-type GST–Syx. Thus, syx^{3} mutants are capable of forming stable core complexes but specifically fail to bind to ROP.

To address the effects of disrupting the Syntaxin–ROP interaction on synaptic transmission, we performed whole-cell patch-clamp analysis at the NMJ. syx^{3} mutants demonstrate a very significantly enhanced evoked junctional current (EJC) amplitude compared to syx^{wt} controls (1.13 ± 0.09 nA for syx^{wt}, n = 19; 2.02 ± 0.11 nA for syx^{3}, n = 8; $p < 0.0001$, Mann-Whitney U test) (Figures 4C and 4D). Two independent transgenic lines show similarly increased evoked responses. To rule out the possibility that the enhancement of evoked response results from a postsynaptic change, we measured the amplitude of spontaneous miniature excitatory junctional currents (mEJCs) (Figure 4E). These data show that quantal size is not significantly altered in syx^{3} mutants (0.19 ± 0.02 nA for syx^{wt}, n = 10; 0.18 ± 0.02 nA

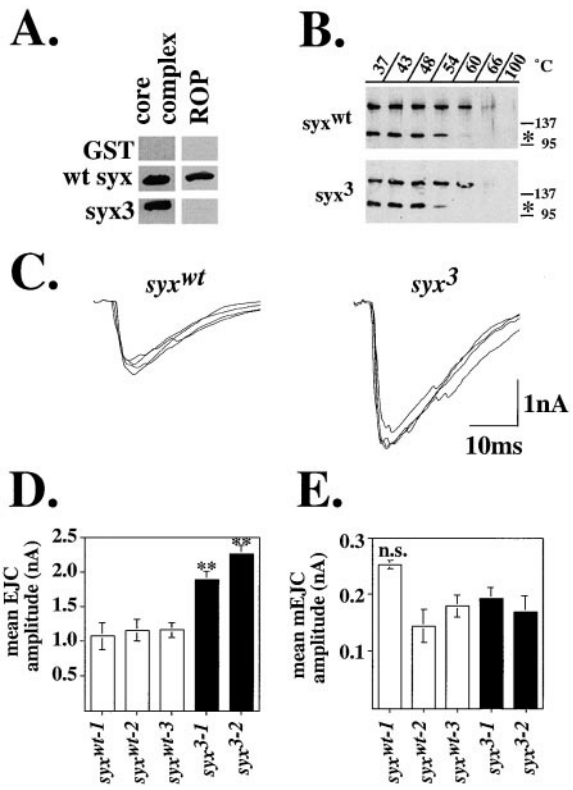

Figure 4. The ROP–Syntaxin Interaction Inhibits Synaptic Transmission

(A) The *syx*^{3} mutation specifically abolishes ROP binding. ROP binding was assessed as described in the Experimental Procedures.

(B) Heat lability of SDS-resistant core complexes formed by GST–Syx or GST–Syx^{3}. The asterisks indicate the size of monomeric core complexes (~115 kD). The higher band likely represents dimeric complexes.

(C) Representative excitatory junctional curents (EJCs) are shown for *syx*^{wt} and for *syx*^{3}.

(D) Mean EJC amplitude for *syx*$^{wt\text{-}1}$ (n = 5), *syx*$^{wt\text{-}2}$ (n = 9), *syx*$^{wt\text{-}3}$ (n = 5), *syx*$^{3\text{-}1}$ (n = 5), and *syx*$^{3\text{-}2}$ (n = 3) embryos are plotted. **p < 0.01.

(E) Mean miniature EJC amplitude is plotted for *syx*$^{wt\text{-}1}$ (n = 3), *syx*$^{wt\text{-}2}$ (n = 4), *syx*$^{wt\text{-}3}$ (n = 4), *syx*$^{3\text{-}1}$ (n = 5), and *syx*$^{3\text{-}2}$ (n = 4) embryos. mEJC amplitude in *syx*$^{wt\text{-}1}$ is not statistically increased compared to other controls or mutants (n.s.).

for *syx*^{3}, n = 9), indicating that the increase in evoked response results from an increase in the number of quanta released. Hence, these data demonstrate that the ROP–Syntaxin complex is not essential for neurotransmission and likely inhibits it.

The Syntaxin–Ca^{2+} Channel Interaction Inhibits Synaptic Transmission

A phenotypic analysis of *syx*^{2}, which specifically impairs synprint binding (Figures 1A and 5A), was conducted to study the function of the Syntaxin–Ca^{2+} channel complex in vivo. To quantitate the reduction of synprint binding to GST–Syx^{2}, we detected bound synprint using ^{125}I-labeled secondary antibodies and phosphorimaging. Binding of the synprint peptide to wild-type GST–Syx is dose dependent and saturable with half-maximal binding at approximately 0.4 μM under these conditions (Figure 5B). GST–Syx^{2} binding to synprint showed an approximately 67% reduction in binding at 1.5 μM synprint compared to wild-type GST–Syx. To rule out the possibility that the *syx*^{2} mutation impairs core complex stability, we tested the heat lability of SDS-resistant core complexes containing GST–Syx^{2}. As shown in Figure 5C, the *syx*^{2} mutation does not affect core complex stability in this assay.

syx^{2} mutants reveal very significantly increased EJC amplitude (1.1 ± 0.1 nA for *syx*^{wt}, n = 19; 2.6 ± 0.2 nA for *syx*^{2}, n = 13; p < 0.0001) (Figures 5D and 5E), compared to *syx*^{wt} controls. Two independent lines, *syx*$^{2\text{-}1}$ and *syx*$^{2\text{-}2}$, have similarly increased EJC amplitudes. To ensure that this increase in evoked response represents a presynaptic phenomenon, we also measured mEJC amplitude. As shown in Figure 5F, mEJC amplitude is not significantly altered in *syx*$^{2\text{-}1}$ or *syx*$^{2\text{-}2}$ mutants, compared to *syx*^{wt} (0.19 ± 0.02 nA for *syx*^{wt}, n = 11; 0.16 ± 0.02 nA for *syx*^{2}, n = 8). Therefore, *syx*^{2} mutants, in which synprint binding is specifically impaired, reveal dramatically increased evoked neurotransmitter release.

In addition to an increase in evoked response, the mEJC frequency is also greatly increased in both *syx*$^{2\text{-}1}$ and *syx*$^{2\text{-}2}$ lines (Figure 5G) (0.25 ± 0.06 mEJCs/s for *syx*^{2} and 0.04 ± 0.01 for *syx*^{wt}; p = 0.0002). At the *Drosophila* embryonic NMJ, a population of mEJC events is Ca^{2+} dependent (Kidokoro and Nishikawa, 1994; Sweeney et al., 1995), and these Ca^{2+}-dependent spontaneous fusions are thought to be triggered by random openings of Ca^{2+} channels. Thus, the increase in mEJC frequency in *syx*^{2} mutants may represent an inability of these mutant Syntaxins to prevent random openings of Ca^{2+} channels. If additional quantal events observed in *syx*^{2} mutants are due to increased openings of Ca^{2+} channels, then, in the absence of Ca^{2+}, the mEJC frequency of *syx*^{2} mutants should be reduced. As shown in Figure 5H, mEJC frequency in *syx*^{2} mutants is significantly reduced in the absence of Ca^{2+} (0.24 ± 0.05 mEJCs/s for *syx*^{2} in 0.5 mM Ca^{2+}, n = 9; 0.12 ± 0.01 for *syx*^{2} in 0 Ca^{2+}, n = 14; p < 0.05). In addition, even in zero Ca^{2+}, *syx*^{2} mutants show significantly more quantal events than *syx*^{wt}, suggesting that the Syntaxin–Ca^{2+} channel interaction also physically inhibits spontaneous fusion in a manner independent of Ca^{2+}. These data suggest that the Syntaxin–Ca^{2+} channel interaction inhibits evoked and spontaneous neurotransmission in vivo.

CSP Binds to the Ca^{2+} Effector Domain of Syntaxin and Is an Effective Competitor of Synprint Binding

Our data suggest that the binding of Syntaxin to presynaptic Ca^{2+} channels inhibits random opening of Ca^{2+} channels. Cysteine string protein (CSP), a synaptic vesicle associated protein, has also been shown to functionally and biochemically interact with Ca^{2+} channels (Gundersen and Umbach, 1992; Leveque et al., 1998). Genetic studies in *Drosophila* suggest that CSP, in concert with other proteins, is required for efficient presynaptic Ca^{2+} entry (Zinsmaier et al., 1994; Umbach et al., 1994, 1998). It is therefore possible that CSP and Syntaxin interact to coordinate Ca^{2+} entry. However, a direct interaction between CSP and Syntaxin has not been reported.

To investigate whether CSP can regulate the Syntaxin–Ca^{2+} channel interaction, we first examined if CSP

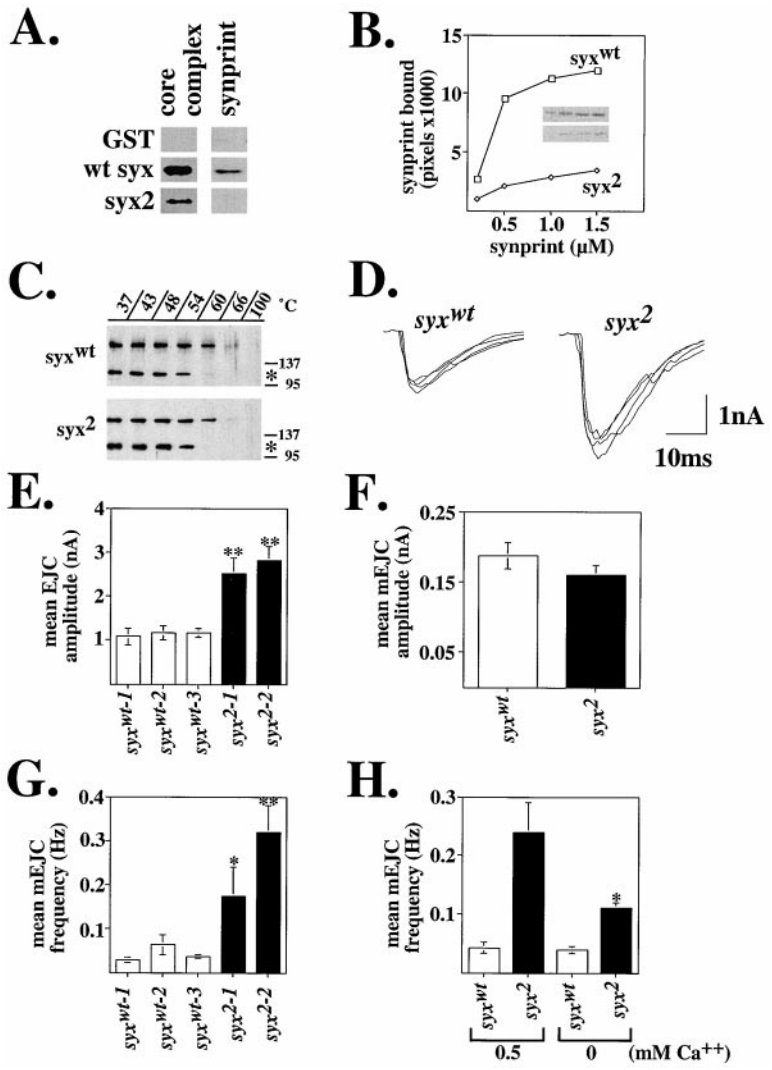

Figure 5. Absence of the Syntaxin–Synprint Interaction Enhances Neurotransmitter Release

(A) The *syx*^{2} mutation abolishes binding to the synprint peptide. Binding of GST fusion proteins to the synprint peptide (amino acids 718–859 N-type Ca^{2+} channel) was performed as described in the Experimental Procedures.

(B) The ability of GST–Syx and GST–Syx^{2} to bind to increasing amounts of synprint peptide was quantitated by phosphorimaging.

(C) Heat lability of SDS-resistant core complexes formed by GST–Syx and GST–Syx^{2} is shown. The asterisks denote the size of the monomeric core complex.

(D) Representative EJCs for *syx*^{wt} and *syx*^{2} embryos.

(E) Mean EJC amplitudes are plotted for *syx*$^{wt\text{-}1}$ (n = 5), *syx*$^{wt\text{-}2}$ (n = 9), *syx*$^{wt\text{-}3}$ (n = 5), *syx*$^{2\text{-}1}$ (n = 7), and *syx*$^{2\text{-}2}$ (n = 6) embryos. **p < 0.01.

(F) Mean miniature EJC (mEJC) amplitudes are plotted for *syx*^{wt} (n = 10) and *syx*^{2} (n = 8). Individual transgenic lines for *syx*^{wt} or *syx*^{2} were not statistically significantly different and thus pooled.

(G) Mean frequency of mEJCs are plotted for *syx*$^{wt\text{-}1}$ (n = 3), *syx*$^{wt\text{-}2}$ (n = 4), *syx*$^{wt\text{-}3}$ (n = 4), *syx*$^{2\text{-}1}$ (n = 5), and *syx*$^{2\text{-}2}$ (n = 4) embryos. *p < 0.05; **p < 0.01.

(H) Mean mEJC frequency are plotted for *syx*^{wt} and *syx*^{2} in 0.5 mM Ca^{2+} or 0 Ca^{2+}. Individual transgenic lines are not statistically different and pooled. Recordings in 0 Ca^{2+} were performed with EGTA, Cd^{2+}, and TTX. Asterisk indicates that mEJC frequency for *syx*^{2} is significantly reduced in the absence of Ca^{2+}; *p < 0.05.

could be found in a complex with Syntaxin. Syntaxin complexes were immunoprecipitated from *Drosophila* head extracts with anti-Syntaxin antibodies (Figure 6A). As shown for vertebrate proteins, *Drosophila* Synaptotagmin could be found to coimmunoprecipitate with Syntaxin (Figure 6A) (Bennett et al., 1992). In addition, we found that CSP also coimmunoprecipitates with Syntaxin. In contrast, two synaptic proteins that do not interact with Syntaxin, Synapsin and SAP47, could not be detected in these immunoprecipitates (data not shown). Since coimmunoprecipitation does not demonstrate direct binding, we also examined whether CSP interacted with Syx in a GST pulldown assay. As shown in Figure 6B, CSP binds to wild-type GST–Syx, but not to GST alone. These data show that CSP can bind directly to Syntaxin in vitro and is present in a complex with Syntaxin in vivo.

As discussed previously, the region deleted in GST–Syx$^{H3\text{-}N}$ is essential for core complex formation and ROP binding, but not Synaptotagmin or synprint binding. Conversely, the region deleted in GST–Syx$^{H3\text{-}C}$ is required for efficient binding to Synaptotagmin and to synprint, but not ROP. To determine if these regions are also important for CSP binding, we tested the ability of CSP to interact with GST–Syx$^{H3\text{-}N}$ and GST–Syx$^{H3\text{-}C}$, as well as GST–Syx^{2} and GST–Syx^{3}. While CSP can interact with GST–Syx$^{H3\text{-}N}$, CSP binding to GST–Syx$^{H3\text{-}C}$ is reduced (Figure 6B). In addition, CSP binds to GST–Syx^{2} and GST–Syx^{3} (data not shown). To quantitate the amount of CSP, Synaptotagmin, and synprint binding to wild-type GST–Syx and GST–Syx$^{H3\text{-}C}$, we performed binding experiments and detected bound proteins using ^{125}I-labeled secondary antibodies and phosphorimaging. Figure 6C shows that binding of CSP to Syntaxin is dose dependent and saturable, with half-maximal binding at approximately 0.2 μM. The apparent stoichiometry of this interaction is approximately 0.3:1 (CSP:GST–Syx), when Syntaxin is immobilized on beads. Maximal binding of CSP to GST–Syx$^{H3\text{-}C}$ is reduced approximately 80%, and the EC_{50} is increased approximately 2-fold, compared to wild-type GST–Syx. As shown in Figure 6D, maximal Synaptotagmin binding to GST–Syx$^{H3\text{-}C}$ is severely reduced using these conditions, compared to wild-type GST–Syx (~90% reduction). In addition, synprint binding to GST–Syx$^{H3\text{-}C}$ is also reduced, relative to wild-type GST–Syx. The *syx*$^{H3\text{-}C}$ deletion causes approximately 85%

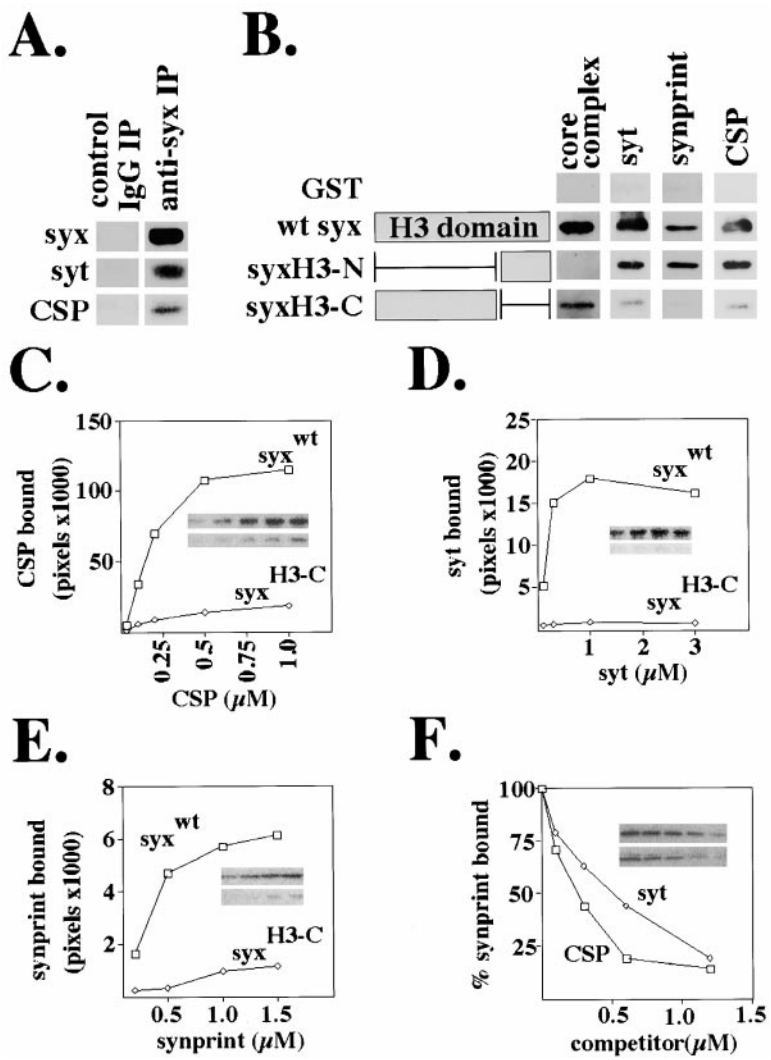

Figure 6. CSP Binds Syntaxin in the Ca^{2+} Effector Domain and Is an Effective Competitor of the Syntaxin–Ca^{2+} Channel Interaction

(A) Immunoprecipitation from *Drosophila* head extracts using either a control antibody (BP104) or anti-syntaxin antibody (8C3).

(B) The Ca^{2+} effector domain (deleted in $syx^{H3\text{-}C}$), but not the core complex domain (deleted in $syx^{H3\text{-}N}$), is required for efficient binding to Synaptotagmin (Syt), synprint, and CSP ($n = 3$).

(C) CSP binds Syntaxin in a dose-dependent and saturable manner. Binding of CSP to immobilized GST–Syx and GST–$Syx^{H3\text{-}C}$ was quantitated by phosphorimaging.

(D) Binding of Synaptotagmin to GST–$Syx^{H3\text{-}C}$ is strongly reduced compared to GST–Syx.

(E) Binding of the synprint peptide to GST–$Syx^{H3\text{-}C}$ is strongly reduced compared to GST–Syx. Although synprint binding to GST–$Syx^{H3\text{-}C}$ appears sigmoid, this may be due to the nonequilibrium binding conditions of these assays.

(F) CSP competes with the Syntaxin–synprint interaction more effectively than Synaptotagmin. Synprint peptide (1 μM) was bound to immobilized GST–Syx (0.30 μM) in the presence of 0, 0.15, 0.3, 0.6, or 1.2 μM CSP or Synaptotagmin. Bound synprint was quantitated by phosphorimaging.

reduction in maximal synprint binding and approximately 2-fold increase in EC_{50} (Figure 6E). Hence, these binding data suggest that the region deleted in $syx^{H3\text{-}C}$ is required for binding of three proteins implicated in Ca^{2+} signaling—CSP, synprint, and Synaptotagmin. We propose that the N-terminal domain of Syntaxin acts as a core domain, while the highly basic C-terminal region of the H3 domain functions as a Ca^{2+} effector domain, spatially localizing proteins required for the production, regulation, and sensing of the Ca^{2+} signal.

A possible model to explain CSP function and its in vitro binding to Syntaxin is that the role of CSP is to alleviate the Syntaxin-mediated inhibition of Ca^{2+} channels, thereby signaling the presence of synaptic vesicles and preparing the machinery for fusion. This model makes a simple prediction, namely that CSP should be able to compete with Syntaxin for the binding to synprint. To test this possibility, immobilized wild-type GST–Syntaxin protein (0.3 μM) was incubated with synprint peptide in the presence of increasing amounts of CSP or Synaptotagmin. Figure 6F shows that CSP effectively competes the Syntaxin–synprint interaction in a dose-dependent manner, with an IC_{50} of approximately 0.3 μM. Synaptotagmin can also compete the Syntaxin–synprint interaction, but somewhat less effectively ($IC_{50} \approx$ 0.6 μM). Therefore, while both CSP and Synaptotagmin can interact with the Ca^{2+} effector domain of Syntaxin, CSP appears to be a more effective competitor of the Syntaxin–synprint interaction than Synaptotagmin. These data further suggest that CSP, Synaptotagmin, and synprint bind to the Ca^{2+} effector domain of Syntaxin. Additionally, these data support the hypothesis that these proteins participate in competitive interactions to regulate Ca^{2+} entry and are consistent with the idea that CSP may disassemble Syntaxin–Ca^{2+} channel complexes by interacting with Syntaxin, the synprint site, or both.

The Ca^{2+} Effector Domain Is Required for Efficient Excitation–Secretion Coupling

We have shown that the Ca^{2+} effector domain binds three proteins implicated in Ca^{2+} signaling. To determine the function of the Ca^{2+} effector domain in neurotransmission, we analyzed the electrophysiological phenotype of $syx^{H3\text{-}C}$ deletion mutants. In the majority (~70%) of mutant animals, evoked transmission is observed, but EJC amplitude is strongly reduced, compared to

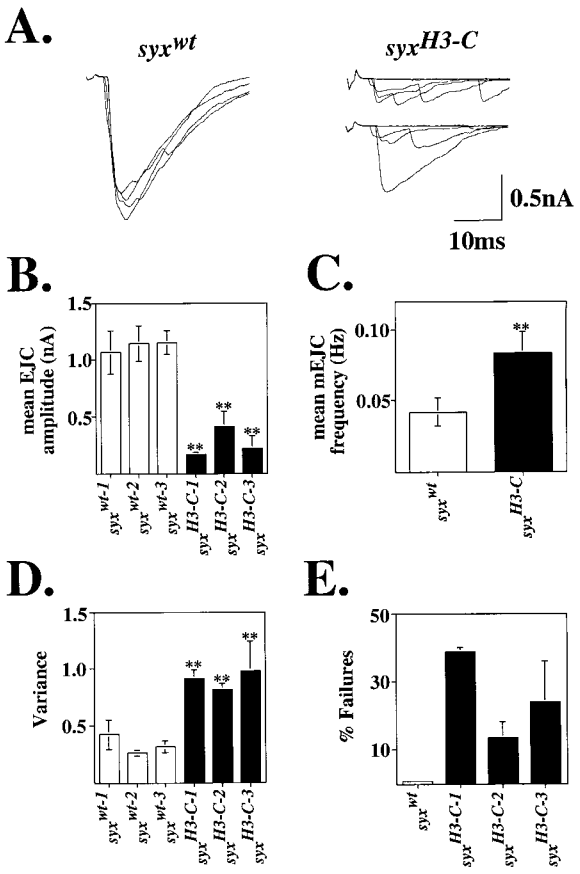

Figure 7. The Ca^{2+} Effector Domain Is Required for Efficient Excitation–Secretion Coupling

(A) Evoked neurotransmitter release in syx^{wt} and $syx^{H3\text{-}C}$ embryos. Traces show representative EJCs after nerve stimulation from these lines. Note that the release for $syx^{H3\text{-}C}$ mutants is asynchronous.

(B) Mean EJC amplitudes of $syx^{wt\text{-}1}$ (n = 5), $syx^{wt\text{-}2}$ (n = 9), $syx^{wt\text{-}3}$ (n = 5), $syx^{H3\text{-}C\text{-}1}$ (n = 3), $syx^{H3\text{-}C\text{-}2}$ (n = 3), and $syx^{H3\text{-}C\text{-}3}$ (n = 2) are plotted. The mean EJC amplitude for $syx^{H3\text{-}C}$ mutants was calculated using animals that showed an evoked response. **$p < 0.01$.

(C) Mean mEJC frequency is plotted for syx^{wt} (n = 19) and $syx^{H3\text{-}C}$ (n = 8) embryos. Data from individual transgenic lines were not statistically different and were thus pooled. **$p < 0.01$.

(D) Evoked neurotransmission is variable in $syx^{H3\text{-}C}$ mutants. Variance of EJC amplitude is plotted (standard deviation/mean EJC amplitude). **$p < 0.01$.

(E) Percentage of failures of evoked response after nerve stimulation in 1.8 mM Ca^{2+}. Individual syx^{wt} transgenic lines were not statistically different and were pooled.

syx^{wt} controls (0.27 ± 0.06 nA for $syx^{H3\text{-}C}$, n = 8; 1.13 ± 0.09 nA for syx^{wt}, n = 19; $p < 0.0001$) (Figures 7A and 7B). In the remaining mutants, evoked secretion was abolished. To control for potential postsynaptic defects, we performed glutamate pressure ejection at $syx^{H3\text{-}C}$ mutant synapses. The mutants reveal robust postsynaptic responses, similar to controls (data not shown). As shown in Figure 7C, mEJC frequency is signficantly increased in $syx^{H3\text{-}C}$ mutants, compared to syx^{wt} controls (0.04 ± 0.01 mEJCs/s for syx^{wt}, n = 11; 0.08 ± 0.01 for $syx^{H3\text{-}C}$, n = 7; p = 0.0083). Thus, in contrast to the complete absence of neurotransmission in $syx^{H3\text{-}N}$ deletion mutants, $syx^{H3\text{-}C}$ deletion mutants reveal strongly reduced evoked responses but an increase in the number of spontaneous quantal events. Both features have been previously associated with *synaptotagmin* mutants (Littleton et al., 1993; Broadie et al., 1994; DiAntonio and Schwarz, 1994).

In addition to a severe reduction of EJC amplitude in $syx^{H3\text{-}C}$ mutants, the mutants also exhibit decreased reliability of excitation–secretion coupling. Specifically, evoked neurotransmission in $syx^{H3\text{-}C}$ mutants is characterized by asynchronous release, low fidelity of release, and a high failure rate (Figure 7). Normally, synchronized fusion of synaptic vesicles is tightly coupled to the Ca^{2+} influx resulting from a single nerve stimulation, and the amount of neurotransmitter released in response to a single stimulation is relatively consistent at the NMJ. However, as shown in Figure 7A, a single stimulation at $syx^{H3\text{-}C}$ synapses can elicit multiple, nonsynchronized EJCs at variable latencies. Furthermore, the variability of release in $syx^{H3\text{-}C}$ mutants is significantly increased compared to syx^{wt} controls (variance of evoked release for syx^{wt} is 0.31 ± 0.04; 0.89 ± 0.06 for $syx^{H3\text{-}C}$; $p < 0.0001$) (Figure 7D). Finally, whereas the NMJs of syx^{wt} animals always release neurotransmitter in response to a nerve stimulation in 1.8 mM extracellular Ca^{2+}, $syx^{H3\text{-}C}$ mutants fail to respond approximately 25% of the time (Figure 7E). Collectively, these phenotypes suggest that loss of the Ca^{2+} effector domain causes defects in the ability of the fusion machinery to properly regulate synchronized release of synaptic vesicles in response to a Ca^{2+} influx. These features are hallmarks of *synaptotagmin* null mutations (Broadie et al., 1994), suggesting that $syx^{H3\text{-}C}$ mutants reveal defects in the sensing of or response to Ca^{2+} in synaptic vesicle fusion.

Discussion

The n-Sec1/ROP-Syntaxin Interaction Is Not Essential for Secretion

Although it is well established that the Sec1 family of proteins can bind to syntaxins, the function of this interaction has been controversial. Because n-Sec1/munc-18 can inhibit core complex formation in vitro, Pevsner et al. (1994b) suggested that this interaction inhibits secretion. However, recent peptide injection studies at the squid giant synapse have suggested an essential role for the syntaxin-s-Sec1 interaction in secretion, as injection of a peptide that inhibits the syntaxin-s-Sec1 interaction in vitro blocks neurotransmitter release (Dresbach et al., 1998). Our finding that the syx^{3} mutation selectively abolishes ROP binding and causes a dramatic increase in evoked neurotransmitter release suggests that the ROP–Syntaxin interaction in vivo is nonessential and inhibitory for neurotransmission (Figure 8). Furthermore, the ROP–Syntaxin interaction is not required in nonneuronal secretion. Although *syx* null and *rop* null embryos fail to secrete cuticle (Harrison et al., 1994; Schulze et al., 1995), syx^{3} mutants are capable of secreting cuticle. These data strongly suggest that the essential functions of both ROP and Syntaxin in nonneuronal secretion are not mediated via a Syntaxin–ROP complex.

Syntaxin Inhibits Synaptic Transmission by Binding Ca^{2+} Channels

Our data suggest that the binding of Syntaxin to the synprint site on Ca^{2+} channels inhibits neurotransmission. We find that *syx* mutations that specifically block

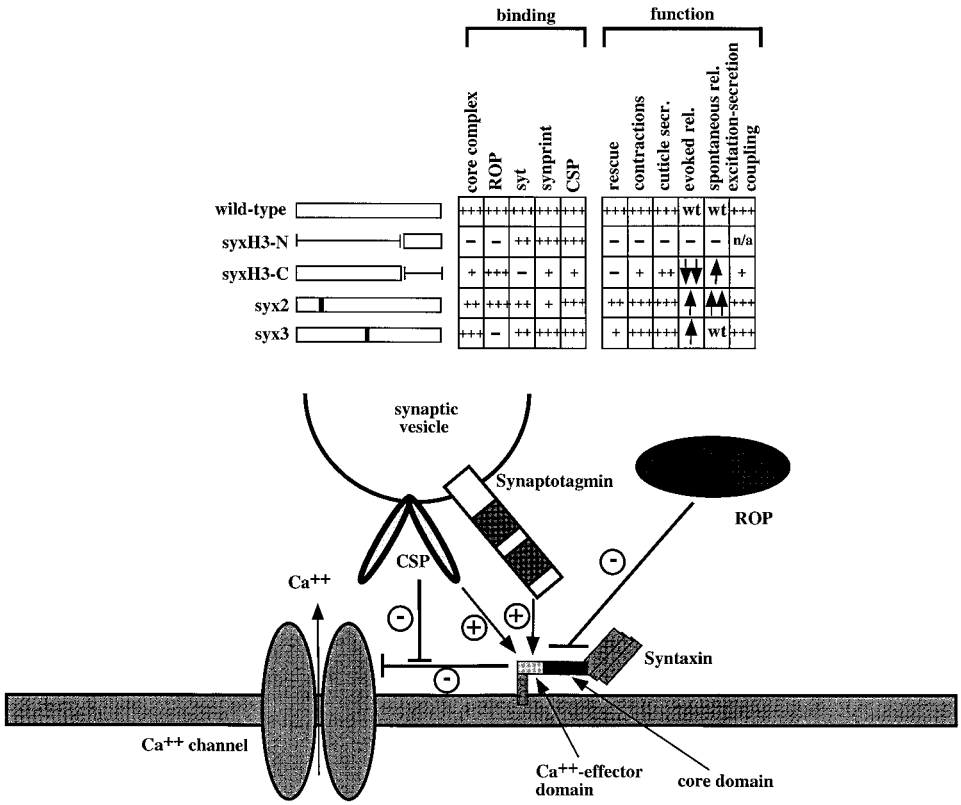

Figure 8. Summary

Binding data are summarized using an arbitrary scale from − (weakest) to +++ (strongest). Functional data are shown using a similar scale or using wt for wild type and arrows indicating an increase or a decrease, relative to controls. Evoked release refers to mean EJC amplitude, while spontaneous release refers to mean mEJC frequency. Below, a schematic is shown, summarizing the data. The H3 domain of Syntaxin consists of a Ca^{2+} effector domain and a core domain. ROP binding to the core domain of Syntaxin is not essential, but rather inhibitory, for synaptic transmission. The Ca^{2+} effector domain binds and spatially organizes CSP, synaptotagmin, and Ca^{2+} channels away from the core domain, which participates in the core complex. The Syntaxin–Ca^{2+} channel interaction is not required for tethering the SV near Ca^{2+} channels, but rather inhibits Ca^{2+} channel openings. CSP may relieve this Syntaxin-mediated inhibition and thus signal the presence of a docked vesicle.

this interaction dramatically increase the amplitude of evoked transmission and also cause an increase in the frequency of spontaneous Ca^{2+}-dependent mEJCs. Importantly, the frequency of spontaneous release at *Drosophila*, rat, and frog NMJs has been shown to be dependent on Ca^{2+}, and this Ca^{2+}-dependent increase in mEJC frequency can be inhibited by Ca^{2+} channel blockers (Grinnell and Pawson, 1989; Kidokoro and Nishikawa, 1994; Sweeney et al., 1995; Losavio and Muchnik, 1997). Taken together, these observations suggest that Syntaxin binding to Ca^{2+} channels reduces both spontaneous and evoked openings of the channels (Figure 8). Our findings do not support an essential function for Syntaxin in tethering the fusion machinery near Ca^{2+} channels, since loss of this function should lead to a reduction in synchronized evoked release. An attractive alternative candidate for such a tethering function is SNAP-25, which has also been shown to bind the synprint site (Sheng et al., 1996).

How are these data reconciled with the observation that injection of synprint peptides into cultured neurons inhibits neurotransmission and causes asynchronous release? In addition to syntaxin, synaptotagmin and CSP have been shown to bind synprint peptides (Sheng et al., 1997; Leveque et al., 1998; Chapman et al., 1999), and our data suggest that the synprint peptide binds to the Ca^{2+} effector domain of Syntaxin. Therefore, one interpretation of these results is that injection of synprint peptides may inhibit the function of these proteins or their interaction with the syntaxin Ca^{2+} effector domain, resulting in a phenotype similar to that observed in $syx^{H3\text{-}C}$ mutants (see below). The syx^{3} and syx^{2} mutations do not appear to alter the stability of their core complexes, suggesting that the structure of the core complex bundle is intact. However, we cannot exclude the possibility that these mutations cause additional defects, such as affecting the conformation or function of the N-terminal domain of Syntaxin, which has been suggested to regulate core complex assembly (Nicholson et al., 1998; Fiebig et al., 1999).

The Core Domain and the Ca^{2+} Effector Domain

The $syx^{H3\text{-}N}$ and $syx^{H3\text{-}C}$ mutants functionally define different regions within the H3 domain: the core domain and the Ca^{2+} effector domain. The core domain is required for core complex assembly, and deletion of this domain shows that the core complex is essential for both nonneuronal and neuronal secretion. In contrast, the $syx^{H3\text{-}C}$ mutant, in which only the Ca^{2+} effector domain is deleted, is capable of nonneuronal secretion, since cuticle

is present in these mutants. Furthermore, the Ca^{2+} effector domain is not required for synaptic vesicle fusion per se, since the frequency of spontaneous synaptic vesicle fusion events is increased in *syx*$^{H3\text{-}C}$ mutants. Rather, the fidelity of evoked Ca^{2+}-dependent neurotransmission is severely affected, suggesting that the Ca^{2+} effector domain plays a specific function in Ca^{2+}-mediated neurotransmission.

We show for the first time that CSP, a protein implicated in regulating Ca^{2+} channels, binds to Syntaxin at its Ca^{2+} effector domain and is an effective competitor of the Syntaxin–synprint interaction. These data suggest that CSP functions to relieve the Syntaxin-mediated inhibition of Ca^{2+} channels. Furthermore, we demonstrate that, in addition to CSP, the Ca^{2+} effector domain of Syntaxin is required for efficient binding of Ca^{2+} channels and Synaptotagmin, which likely functions as a Ca^{2+} sensor (Figure 8). The observation that three key Ca^{2+}-signaling proteins bind to the C-terminal region of the H3 domain suggests that this region is critical for mediating Ca^{2+}-dependent excitation–secretion coupling. These binding data lead to two simple predictions. First, in the absence of CSP, Ca^{2+} entry should be reduced as Syntaxin may partially block Ca^{2+} entry. This is in agreement with the phenotype observed in CSP mutants (Umbach et al., 1998). Since the *csp* mutant phenotype worsens with elevated temperature, it is possible that another protein may partially substitute for CSP function at room temperature (Zinsmaier et al., 1994; Umbach et al., 1998). Second, deletion of the Ca^{2+} effector domain of Syntaxin should effectively uncouple Ca^{2+} entry and evoked response, but not abolish fusion, that is, cause a phenotype similar to the absence of Synaptotagmin. This phenotype is indeed observed in *syx*$^{H3\text{-}C}$ mutants.

Our electrophysiological studies show that deletion of the Ca^{2+} effector domain causes a severe reduction in Ca^{2+}-dependent evoked neurotransmission, but an increase in spontaneous vesicle fusion. Furthermore, the reliability of excitation–secretion coupling is severely impaired, as evoked neurotransmission in *syx*$^{H3\text{-}C}$ mutants is characterized by asynchronous, low-fidelity, and high-failure release. These characteristics are not caused by lower levels of Syx$^{H3\text{-}C}$ protein, since a *syx* hypomorph (*P1697*), which expresses wild-type Syntaxin at levels very similar to *syx*$^{H3\text{-}C}$ mutants, does not exhibit these phenotypes (Schulze et al., 1995). Asynchronous, low-fidelity, and high-failure release are hallmarks of *synaptotagmin* null mutants in *Drosophila* (Broadie et al., 1994) and, combined with the reduction of Synaptotagmin binding to GST–Syx$^{H3\text{-}C}$, strongly suggest that Synaptotagmin meditates its Ca^{2+}-sensing function through Syntaxin. To date, there is only one other *Drosophila* gene whose mutation causes a similar phenotype: *stoned* (Stimson et al., 1998; Fergestad et al., 1999). However, since Synaptotagmin is mislocalized in these mutants, it is likely that this phenotype reflects a loss of Synaptotagmin function (Fergestad et al., 1999). Taken together, these data suggest that the Ca^{2+} effector domain functions in the fast, synchronized response to a Ca^{2+} influx via an interaction with Synaptotagmin. Alternatively, it is possible that the phenotype caused by the *syx*$^{H3\text{-}C}$ deletion is due to reducing the distance between the transmembrane domain and the core complex bundle. However, the *syx*$^{H3\text{-}C}$ deletion does not generally impair core complex function in fusion, since the frequency of spontaneous fusion events is increased in *syx*$^{H3\text{-}C}$ mutants, implying that in this alternate scenario, the distance between the transmembrane domain and the core complex bundle is specifically important for evoked neurotransmission.

Our studies of targeted mutations in Syntaxin have dissected different regulatory functions of Syntaxin in neuronal and nonneuronal secretion. Furthermore, we have characterized a novel domain within Syntaxin that likely coordinates Ca^{2+} triggering of synaptic vesicle exocytosis, providing a mechanism for CSP function and for spatially organizing Ca^{2+}-related steps of exocytosis. With the increasing availability of structural information about proteins implicated in synaptic vesicle exocytosis, future targeted mutational analyses in vivo should continue to yield important insights into the mechanisms of neurotransmitter release.

Experimental Procedures

Generation of Syntaxin Mutant Rescue Constructs and Transgenic Lines

A genomic rescue construct was generated by subcloning a 13.5 kb XbaI fragment from λ6 (Schulze et al., 1995), containing the entire *syx* cDNA into pCasper3. Deletions in the *syx* ORF removing amino acids 204–250 (*syx*$^{H3\text{-}N}$ deletion) and 253–267 (*syx*$^{H3\text{-}C}$ deletion) were made by using high-fidelity PCR (XL-PCR Kit [Perkin-Elmer]) with outward facing primers, whose ends produce a novel restriction site (BglII). To generate point mutations within the *syx* ORF, the Quikchange kit (Stratagene) was used as described by manufacturer to mutate I212A (*syx*^{2}) and I236A (*syx*^{3}). All mutant constructs were sequenced to confirm the presence of point mutations and absence of inadvertent mutations.

Transgenic lines bearing these constructs were generated as described (Rubin and Spradling, 1982). These transgenic lines were then crossed into either the null *syx*^{229} background or hypomorphic *syx*^{P1697} background and balanced over *TM6B, Tb Hu* (Lindsley and Zimm, 1992) or *TM3, Kr GFP* (a gift of D. Casso and T. Kornberg), in order to identify mutant embryos and larvae. All fly strains were maintained at room temperature on standard cornmeal–molasses medium. Mutant embryos were identified by using either a GFP balancer or by using strains that were outcrossed to wild-type flies such that all nonhatchers were mutant. Cuticles were examined by preparing as described in Ashburner (1990) and using darkfield microscopy (10×, Zeiss Axiophot). Single embryo Westerns were performed as described (Harrison et al., 1994).

Immunoprecipitations

Flies were frozen in liquid N_2, and heads were collected with a sieve. For every 1 mL of heads, 2 mL of buffer K (50 mM KCl and 10 mM HEPES [pH 7.0]) were used with 0.1 mM PMSF. Heads were crushed with a mortar and pestle and then homogenized using a Dounce homogenizer. Cuticular debris was pelleted at 1000 × g. Supernatant (0.5 mL, approximately 500 μg protein) was incubated with 200 μl of 8C3 anti-Syx antibody or, as a negative control, an unrelated monoclonal antibody (BP104) with 0.2% Tx-100 O/N at 4°C. Insoluble material was spun down 10× at 16,000 × g. The supernatant was incubated with protein A–agarose beads (GIBCO) for 2 hr at 4°C. The beads were washed 4 × 1 mL buffer K and bound proteins were released by boiling in SDS sample buffer. 49/92 (anti-csp) was used at 1:10,000 and 8C3 (anti-syx) was used at 1:1,000.

Preparation of Recombinant Proteins

For GST–Syx protein constructs, aa (amino acids) 1–272 were subcloned into pGEX-4T (Pharmacia). pGEX-Syt construct (aa 134–474) was provided by J. T. Littleton. The *SNAP-25* ORF was subcloned using EcoRI/XhoI into pET28c (Novagen). *n-syb* (aa 1–104) was subcloned using BamHI/NdeI into pET28a. The His–synprint (N-type Ca^{2+} channel) construct (aa 718–859) was provided by W. Caterall.

The entire *csp* ORF was digested with BamHI/EcoRI and subcloned into pET-28c. GST fusion or His-tagged proteins were purified as described by manufacturer (Pharmacia or Novagen). The GST tag was thrombin cleaved from GST–Synaptotagmin using manufacturer's protocol (Pharmacia). To change buffers, proteins were concentrated using Centriprep columns (Amicon) and washed twice with 10 mL of PBS (140 mM NaCl, 2.7 mM KCl, 10.1 mM Na_2HPO_4, 1.8 mM KH_2PO_4 [pH 7.3]). Protein concentrations were estimated by Coomassie blue staining of protein bands after SDS-PAGE using bovine serum albumin as a standard.

In Vitro Binding Assays and Competition Assays

All proteins used in these assays were *Drosophila* proteins, with the exception of the rat synprint peptide. Binding was performed essentially as described (Kee et al., 1995). Similar data were observed for both Synaptotagmin and synprint in the presence and absence of 1 mM Ca^{2+}, except that signals were stronger in the presence of Ca^{2+} (data not shown). Because Synaptotagmin and cysteine string protein bound nonspecifically to the glutathione Sepharose beads, 20–100 μg of bacterial extract was used in these binding assays as a nonspecific competitor (Assubel, 1996). To assess the ability of the ternary core complex to form with mutant Syntaxin proteins, both Syb and SNAP-25 were allowed to bind to GST–Syx O/N. For competition assays, the ability of His–synprint to bind to GST–Syx was assessed in the presence of 0, 0.15, 0.3, 0.6, and 1.2 μM CSP or Synaptotagmin. CSP or Synaptotagmin was added after 1 hr; otherwise, the binding assay was performed as above. Since we were unable to produce soluble full-length ROP, we detected the Syx–ROP interaction by performing GST pulldown experiments using head extracts, as described (Littleton et al., 1998). Proteins on beads were released by boiling in 20 μL sample buffer and subjected to SDS-PAGE and Western blotting. Proteins were detected using antibodies as described in Schulze et al. (1995). To detect synprint, anti-express antibody (Invitrogen, 1:5000) was used. For dose-response binding curves, binding experiments were performed as above, except that increasing amounts of target proteins were used (in μM): synprint, 0.2, 0.5, 1, 1.5; CSP, 0.03, 0.1, 0.2, 0.5, 1; synaptotagmin, 0.1, 0.3, 1, 3. Bands were detected by ^{125}I-labeled secondary antibodies at 1:1000 (Amersham), quantitated by phosphorimaging (Storm860 [Molecular Dynamics]), and analyzed by ImageQuant software (Molecular Dynamics). Analysis of SDS-resistant core complexes was performed as in Hayashi et al. (1994), except that samples were incubated for 5′ at 37°C, 43°C, 48°C, 54°C, 60°C, 66°C, or 100°C. Bands were detected with a polyclonal n-syb antibody (R29) at 1:2000 using ECL. R29 was generated by injecting the full-length cytoplasmic domain of *Drosophila* n-Syb into a rat, using standard protocols (Cocalico Biologicals).

Electrophysiology

Electrophysiological recordings were performed as previously reported (Broadie and Bate, 1993). Selected embryos were dissected in standard *Drosophila* saline at 22–24 hr after fertilization (incubated at 25°C). All recordings were made at 18°C using standard whole-cell patch-clamp (−60 mV) techniques. Recordings were taken from muscle 6 in anterior abdominal segments A2–A3. EJCs were evoked by brief stimulation of the motor nerve (1 ms) with positive current using a glass suction electrode. Mean EJC amplitudes were determined from 25 consecutive EJCs evoked at each frequency. Data were acquired and analyzed using pCLAMP 6.0 software (Axon Instruments). mEJCs were acquired from at least five animals. Standard mEJC recordings were done in 0.1 μM TTX (Sigma) at 0.5 mM external calcium. Calcium-free mEJC recordings were done in normal bath saline with no Ca^{2+}, 0.1 μM TTX, 100 μM Cd^{2+}, and 0.1 mM EGTA. mEJC amplitude and frequency were analyzed using Mini Analysis software 3.0 (Jaejin Software). Statistical analyses were done with Instat (Graphpad software). All significance values were calculated using Mann-Whitney U tests. Error is expressed as SEM.

Acknowledgments

We thank G. Bhave and K. Schulze for help with binding assays. We are grateful to D. Casso and T. Kornberg for sharing their Kr GFP balancer flies with us prior to publication. We thank J. Roos, R. Kelly, T. Südhof, R. Jahn, and K. Zinsmaier for providing antibodies. We also thank T. Schwarz, B. McCabe, C. O'Kane, J. T. Littleton, W. Caterall, and K. Zinsmaier for providing DNA constructs. For the protocol for coimmunoprecipitation of CSP and Syx, we thank J. Wenniger and K. Zinsmaier. We thank M. L. Zhao for help with calcium-free recordings. We thank A. Bean, E. Chapman, and B. Dickey for helpful comments and advice on this manuscript. We also acknowledge members of the Bellen and Broadie labs for critically reading this manuscript. M. N. W. and T. E. L. are supported by predoctoral NIMH National Research Service Award training grants. T. F. is supported by an NIH Developmental Biology Training Grant, and K. B. is funded by the NIH (GM54544) and a Searle Scholarship. This work was supported by an NIH grant to H. J. B. and by the Howard Hughes Medical Institute (HHMI). H. J. B. is an associate investigator of the HHMI.

Received May 7, 1999; revised June 15, 1999.

References

Ashburner, M. (1990). Drosophila: A Laboratory Handbook (Cold Spring Harbor, NY: Cold Spring Harbor Laboratory Press).

Assubel, F. (1996). Analysis of protein interactions. In Current Protocols in Molecular Biology, V. Chanda, ed. (New York: John Wiley and Sons).

Bajjalieh, S.M., and Scheller, R.H. (1995). The biochemistry of neurotransmitter secretion. J. Biol. Chem. *270*, 1971–1974.

Bennett, M.K., Calakos, N., and Scheller, R.H. (1992). Syntaxin: a synaptic protein implicated in docking of synaptic vesicles at presynaptic active zones. Science *257*, 255–259.

Betz, A., Okamoto, M., Benseler, F., and Brose, N. (1997). Direct interaction of the rat unc-13 homologue Munc13–1 with the N terminus of syntaxin. J. Biol. Chem. *272*, 2520–2526.

Bezprozvanny, L., Scheller, R.H., and Tsien, R.W. (1995). Functional impact of syntaxin on gating of N-type and Q-type calcium channels. Nature *378*, 623–626.

Broadie, K.S., and Bate, M. (1993). Development of the embryonic neuromuscular synapse of *Drosophila melanogaster*. J. Neurosci. *13*, 144–166.

Broadie, K., Bellen, H.J., DiAntonio, A., Littleton, J.T., and Schwarz, T.L. (1994). The absence of synaptotagmin disrupts excitation–secretion coupling during synaptic transmission. Proc. Natl. Acad. Sci. USA *91*, 10727–10731.

Broadie, K., Prokop, A., Bellen, H.J., O'Kane, C.J., Schulze, K.L., and Sweeney, S.T. (1995). Syntaxin and synaptobrevin function downstream of vesicle docking in *Drosophila*. Neuron *15*, 663–673.

Brown, K.A., Howell, E.E., and Kraut, J. (1993). Long-range structural effects in a second-site revertant of a mutant dihydrofolate reductase. Proc. Natl. Acad. Sci. USA *90*, 11753–11756.

Chapman, E.R., An, S., Barton, N., and Jahn, R. (1994). SNAP-25, a t-SNARE which binds to both syntaxin and synaptobrevin via domains that may form coiled coils. J. Biol. Chem. *269*, 27427–27432.

Chapman, E.R., Hanson, P.I., An, S., and Jahn, R. (1995). Ca^{2+} regulates the interaction between synaptotagmin and syntaxin 1. J. Biol. Chem. *270*, 23667–23671.

Chapman, E.R., Desai, R.C., Davis, A.F., and Tornehl, C.K. (1999). Delineation of the oligomerization, AP-2 binding, and synprint binding region of the C2B domain of synaptotagmin. J. Biol. Chem. *273*, 32966–32972.

Chen, Y.A., Scales, S.J., Patel, S.M., Doung, Y.-C., and Scheller, R.H. (1999). SNARE complex formation is triggered by Ca^{2+} and drives membrane fusion. Cell *97*, 165–174.

DiAntonio, A., and Schwarz, T.L. (1994). The effect on synaptic physiology of synaptotagmin mutations in *Drosophila*. Neuron *12*, 909–920.

Dresbach, T., Burns, M.E., O'Connor, V., DeBello, W.M., Betz, H., and Augustine, G.J. (1998). A neuronal Sec1 homolog regulates neurotransmitter release at the squid giant synapse. J. Neurosci. *18*, 2923–2932.

Fergestad, T., Davis, W.S., and Broadie, K. (1999). The stoned proteins regulate synaptic vesicle recycling in the presynaptic terminal. J. Neurosci., in press.

Fernandez, I., Ubach, J., Dulubova, I., Zhang, X., Südhof, T.C., and Rizo, J. (1998). Three-dimensional structure of an evolutionarily conserved N-terminal domain of syntaxin 1A. Cell *94*, 841–849.

Fiebig, K.M., Rice, L.M., Pollock, E., and Brunger, A.T. (1999). Folding intermediates of SNARE complex assembly. Nat. Struct. Biol. *6*, 117–123.

Fisher, B.M., Schultz, L.W., and Raines, R.T. (1998). Coulombic effects of remote sites on the active site of ribonuclease A. Biochemistry *37*, 17386–17401.

Fujita, Y., Shirataki, H., Sakisaka, T., Asakura, T., Ohya, T., Kotani, H., Yokoyama, S., Nishioka, H., Matsuura, Y., Mizoguchi, A., et al. (1998). Tomosyn: a syntaxin-1-binding protein that forms a novel complex in the neurotransmitter release process. Neuron *20*, 905–915.

Grinnell, A.D., and Pawson, P.A. (1989). Dependence of spontaneous release at frog junctions on synaptic strength, external calcium, and terminal length. J. Physiol. (Lond.) *418*, 397–410.

Gundersen, C.B., and Umbach, J.A. (1992). Suppression cloning of the cDNA encoding a candidate subunit of a presynaptic calcium channel. Neuron *9*, 527–537.

Hanson, P.I., Roth, R., Morisaki, H., Jahn, R., and Heuser, J.E. (1997). Structure and conformational changes in NSF and its membrane receptor complexes visualized by quick-freeze/deep-etch electron microscopy. Cell *90*, 523–535.

Harrison, S.D., Broadie, K., van de Goor, J., and Rubin, G.M. (1994). Mutations in the *Drosophila Rop* gene suggest a function in general secretion and synaptic transmission. Neuron *13*, 555–566.

Hata, Y., Slaughter, C.A., and Südhof, T.C. (1993). Synaptic vesicle fusion complex contains *unc-18* homologue bound to syntaxin. Nature *366*, 347–351.

Hayashi, T., McMahon, H., Yamasaki, S., Binz, T., Hata, Y., Südhof, T.C., and Niemann, H. (1994). Synaptic vesicle membrane fusion complex: action of clostridial neurotoxins on assembly. EMBO J. *13*, 5051–5061.

Hsu, S.C., Ting, A.E., Hazuka, C.D., Davanger, S., Kenny, J.W., Kee, Y., and Scheller, R.H. (1996). The mammalian brain rsec6/8 complex. Neuron *17*, 1209–1219.

Hunt, J.M., Charlton, M.P., Kistner, A., Habermann, E., Augustine, G.J., and Betz, H. (1994). A post-docking role for synaptobrevin in synaptic vesicle fusion. Neuron *12*, 1269–1279.

Jahn, R., and Hanson, P.I. (1998). Membrane fusion. SNAREs line up in new environment. Nature *393*, 14–15.

Kee, Y., Lin, R.C., Hsu, S.-C., and Scheller, R.H. (1995). Distinct domains of syntaxin are required for synaptic vesicle fusion complex formation and dissociation. Neuron *14*, 991–998.

Kidokoro, Y., and Nishikawa, K. (1994). Miniature endplate currents at the newly formed neuromuscular junction in Drosophila embryos and larvae. Neurosci. Res. *19*, 143–154.

Krasnoperov, V.G., Bittner, M.A., Beavis, R., Kuang, Y., Salnikow, K.V., Chepurny, O.G., Little, A.R., Plotnikov, A.N., Wu, D., Holz, R.W., and Petrenko, A.G. (1997). α-latrotoxin stimulates exocytosis by the interaction with a neuronal G-protein-coupled receptor. Neuron *18*, 925–937.

Leveque, C., Pupier, S., Marqueze, B., Geslin, L., Kataoka, M., Takahashi, M., De Waard, M., and Seagar, M. (1998). Interaction of cysteine string proteins with the alpha1A subunit of the P/Q-type calcium channel. J. Biol. Chem. *273*, 13488–13492.

Lin, R.C., and Scheller, R.H. (1997). Structural organization of the synaptic exocytosis core complex. Neuron *19*, 1087–1094.

Lindsley, D.L., and Zimm, G.G. (1992). The Genome of *Drosophila melanogaster* (New York: Academic Press).

Littleton, J.T., Stern, M., Schulze, K., Perin, M., and Bellen, H.J. (1993). Mutational analysis of *Drosophila synaptotagmin* demonstrates its essential role in Ca^{2+}-activated neurotransmitter release. Cell *74*, 1125–1134.

Littleton, J.T., Chapman, E.R., Kreber, R., Garment, M.B., Carlson, S.D., and Ganetzky, B. (1998). Temperature-sensitive paralytic mutations demonstrate that synaptic exocytosis requires SNARE complex assembly and disassembly. Neuron *21*, 401–413.

Losavio, L., and Muchnik, S. (1997). Spontaneous acetylcholine release in mammalian neuromuscular junctions. Am. J. Physiol. *273*, C1835–C1841.

Marsal, J., Ruiz-Montasell, B., Blasi, J., Moreira, J.E., Contreras, D., Sugimori, M., and Llinas, R. (1997). Block of transmitter release by botulinum C1 action on syntaxin at the squid giant synapse. Proc. Natl. Acad. Sci. USA *94*, 14871–14876.

Martinez Arias, A. (1993). Development and patterning of the larval epidermis of *Drosophila*. In The Development of *Drosophila*, M. Bate and A. Martinez Arias, eds. (New York: Cold Spring Harbor Press), pp. 517–608.

McMahon, H.T., Missler, M., Li, C., and Südhof, T.C. (1995). Complexins: cytosolic proteins that regulate SNAP receptor function. Cell *83*, 111–119.

Mochida, S., Sheng, Z.H., Baker, C., Kobayashi, H., and Catterall, W.A. (1996). Inhibition of neurotransmission by peptides containing the synaptic protein interaction site of N-type Ca^{2+} channels. Neuron *17*, 781–788.

Nichols, B.J., Ungermann, C., Pelham, H.R.B., Wickner, W.T., and Haas, A. (1997). Homotypic vacuolar fusion mediated by t- and v-SNAREs. Nature *387*, 199–202.

Nicholson, K.L., Munson, M., Miller, R.B., Filip, T.J., Fairman, R., Hughson, F.M. (1998). Regulation of SNARE complex assembly by an N-terminal domain of the t-SNARE Sso1p. Nat. Struct. Biol. *5*, 793–802.

Novick, P., Field, C., and Schekman, R. (1980). Identification of 23 complementation groups required for post-translational events in the yeast secretory pathway. Cell *21*, 205–215.

O'Connor, V., Heuss, C., De Bello, W.M., Dresbach, T., Charlton, M.P., Hunt, J.H., Pellegrini, L.L., Hodel, A., Burger, M.M., Betz, H., Augustine, G.J., and Schafer, T. (1997). Disruption of syntaxin-mediated protein interactions blocks neurotransmitter secretion. Proc. Natl. Acad. Sci. USA *94*, 12186–12196.

Pevsner, J., Hsu, S.-C., and Scheller, R. (1994a). n-Sec1: a neural-specific syntaxin-binding protein. Proc. Natl. Acad. Sci. USA *91*, 1445–1449.

Pevsner, J., Hsu, S.-C., Braun, J.E.A., Calakos, N., Ting, A.E., Bennett, M.K., and Scheller, R.H. (1994b). Specificity and regulation of a synaptic vesicle docking complex. Neuron *13*, 353–361.

Rettig, J., Heinemann, C., Ashery, U., Sheng, Z.H., Yokoyama, C.T., Catterall, W.A., and Neher, E. (1997). Alteration of Ca^{2+} dependence of neurotransmitter release by disruption of Ca^{2+} channel/syntaxin interation. J. Neurosci. *17*, 6647–6656.

Rubin, G.M., and Spradling, A.C. (1982). Genetic transformation of *Drosophila* with transposable element vectors. Science *218*, 348–353.

Saifee, O., Wei, L., and Nonet, M.L. (1998). The *Caenorhabditis elegans* unc-64 locus encodes a syntaxin that interacts genetically with synaptobrevin. Mol. Biol. Cell *9*, 1235–1252.

Schulze, K.L., and Bellen, H.J. (1996). *Drosophila syntaxin* is required for cell viability and may function in membrane formation and stabilization. Genetics *144*, 1713–1724.

Schulze, K.L., Littleton, J.T., Salzberg, A., Halachmi, N., Stern, M., Lev, Z., and Bellen, H.J. (1994). *rop*, a *Drosophila* homolog of yeast Sec1 and vertebrate n-Sec1/Munc-18 proteins, is a negative regulator of neurotransmitter release in vivo. Neuron *13*, 1099–1108.

Schulze, K.L., Broadie, K., Perin, M.S., and Bellen, H.J. (1995). Genetic and electrophysiological studies of *Drosophila* syntaxin-1A demonstrate its role in nonneuronal secretion and neurotransmission. Cell *80*, 311–320.

Sheng, Z.H., Rettig, J., Takahashi, M., and Catterall, W.A. (1994). Identification of a syntaxin-binding site on N-type calcium channels. Neuron *13*, 1303–1313.

Sheng, Z.H., Rettig, J., Cook, T., and Catterall, W.A. (1996). Calcium-dependent interaction of N-type calcium channels with the synaptic core complex. Nature *379*, 451–454.

Sheng, Z.H., Yokoyama, C.T., and Catterall, W.A. (1997). Interaction

of the synprint site of N-type Ca^{2+} channels with the C2B domain of synaptotagmin I. Proc. Natl. Acad. Sci. USA *94*, 5405–5410.

Sollner, T., Whiteheart, S.W., Brunner, M., Erdjument-Bromage, H., Geromanos, S., Tempst, P., and Rothman, J.E. (1993a). SNAP receptors implicated in vesicle targeting and fusion. Nature *362*, 318–324.

Sollner, T., Bennett, M.K., Whiteheart, S.W., Scheller, R.H., and Rothman, J.E. (1993b). A protein assembly-disassembly pathway in vitro that may correspond to sequential steps of synaptic vesicle docking, activation, and fusion. Cell *75*, 409–418.

Stimson, D.T., Estes, P.S., Smith, M., Kelly, L.E., and Ramaswami, M. (1998). A product of the *Drosophila* stoned locus regulates neurotransmitter release. J. Neurosci. *18*, 9638–9649.

Sugimori, M., Tong, C.K., Fukuda, M., Moreira, J.E., Kojima, T., Mikoshiba, K., and Llinas, R. (1998). Presynaptic injection of syntaxin-specific antibodies blocks transmission in the squid giant synapse. Neurosci. *86*, 39–51.

Sutton, R.B., Fasshauer, D., Jahn, R., and Brunger, A.T. (1998). Crystal structure of a SNARE complex involved in synaptic exocytosis at 2.4 A resolution. Nature *395*, 347–353.

Sweeney, S.T., Broadie, K., Keane, J., Niemann, H., and O'Kane, C.J. (1995). Targeted expression of tetanus toxin light chain in *Drosophila* specifically eliminates synaptic transmission and causes behavioral defects. Neuron *14*, 341–351.

Umbach, J.A., Zinsmaier, K.E., Eberle, K.K., Buchner, E., Benzer, S., and Gundersen, C.B. (1994). Presynaptic dysfunction in *Drosophila csp* mutants. Neuron *13*, 899–907.

Umbach, J.A., Saitoe, M., Kidokoro, Y., and Gundersen, C.B. (1998). Attenuated influx of calcium ions at nerve endings of *csp* and *shibire* mutant *Drosophila*. J. Neurosci. *18*, 3233–3240.

Weber, T., Zemelman, B.V., McNew, J.A., Westermann, B., Gmachl, M., Parlati, F., Sollner, T.H., and Rothman, J.E. (1998). SNAREpins: minimal machinery for membrane fusion. Cell *92*, 759–772.

Wiser, O., Bennett, M.K., and Atlas, D. (1996). Functional interaction of syntaxin and SNAP-25 with voltage-sensitive L- and N-type Ca^{2+} channels. EMBO J. *15*, 4100–4110.

Wu, M.N., Littleton, J.T., Bhat, M.A., Prokop, A., and Bellen, H.J. (1998). ROP, the *Drosophila* Sec1 homolog, interacts with syntaxin and regulates neurotransmitter release in a dosage-dependent manner. EMBO J. *17*, 127–139.

Zinsmaier, K.E., Eberle, K.K., Buchner, E., Walter, N., and Benzer, S. (1994). Paralysis and early death in cysteine string protein mutants of *Drosophila*. Science *263*, 977–980.